

Different Local Binary Operators for Texture Classification: A Comparative Study



Abeer Shamaileh¹, Taha H. Rassem^{*2}, Liew Siau Chuin³, Osama Nayel Al Sayaydeh⁴

^{1,2,3 & 4} Faculty of Computer Systems and Software Engineering, Universiti Malaysia Pahang, Malaysia

*tahahusseini@ump.edu.my

ABSTRACT

Local Binary Patterns (LBP) have brightened up as one of the most eminent and widely studied texture descriptors. LBP has gained high acceptance due to its simplicity, high distinguishing power, and flexibility. As such, it has been deployed in several applications where it has performed well. This is why LBP is the basis for a new research direction. However, LBP has limitations that may affect its accuracy. Therefore, many descriptors based on LBP have been proposed to overcome its limitations and enhance its accuracy, such as Local Ternary Pattern (LTP), Completed Local Binary Pattern (CLBP), Completed Local Binary Count (CLBC), Completed Local Ternary Pattern (CLTP), and Wavelet Completed Local Ternary Pattern (WCLTP). This paper is focused to provide a comparative analysis by studying and evaluating the performance of LBP descriptor and five of its variants using three well-known benchmark texture datasets. Furthermore, this study also seeks to improve the role of image texture information in classification processes. Different experiments were conducted using three benchmark texture datasets which are CURET, OuTeX and UIUC. The experimental results showed that WCLTP outperformed other texture descriptors and achieved the highest classification accuracy in all experiments. WCLTP achieved 99.35%, 96.57% and 94.80% classification accuracy with CURET and OuTeX and UIUC respectively.

Key words : LBP; Texture classification; Texture descriptor; Outex dataset; CURET dataset.

1. INTRODUCTION

The texture is an essential characteristic of images because it represents an enormous source of information about the image. It can be utilized to separate one image from another. In recent times, texture classification recognized as one of the significant issues in the texture analysis field. It has received impressive consideration due of its vital role in several applications for image analysis, such as medical images analysis [1], object recognition [2], face recognition [3], and image retrieval [4]. Texture classification includes four main steps which are preprocessing, feature extraction, feature selection, and classification. Many researchers agree that the

feature extraction step is the most important step because the powerful extracted features play a crucial role in the final classification results. However, if the best classifier is fed by weak features, then it will fail to achieve good result [5]. Therefore, several texture descriptors have been proposed to obtain an efficient texture classification. The main purpose of these texture descriptors is how to extract distinctive texture features that are robust to image effects such as noise, rotation, blurriness, and illumination variance. These descriptors can be categorized into four main groups [6]. The first group is the structural methods such as fractal analysis [7]. The second group is the model-based methods such as the Markov Random Field (MRF) [8]. The third group is the Transform-based methods such as wavelet transform [9]. The fourth group is the statistical methods such as Local Binary Patterns (LBP) [10]. LBP is one of the effective proposed texture descriptors. The basic concept of LBP is that an image is structured from micropatterns. The absolute difference between the gray level of the center pixel of each pattern and its neighbors are used to construct the histogram. The histogram of these micropatterns holds information about the distribution of image features such as edges, spots, and lines. LBP received wide popularity because it has distinctive characteristics such as computational simplicity, flexibility, high distinguishing ability, and invariance against monotonic grey level changes. Therefore, it has been deployed in several applications and has achieved good performance records. However, the most serious disadvantages of LBP are its high sensitivity to noise and sometimes the different patterns of LBP possibly could be classified into the same class. Thus, many different variants of LBP have been proposed to improve its discriminative power for texture classification and overcome its limitations. Several literature surveys on different variants of LBP methods have been conducted [11] [12] [13]; however, they missed some of the important recent variants such as CLTP and WCLTP, and the experimental evaluations are missing too. In this paper, a review of the LBP descriptor and some of its well-known variants (i.e. LTP, CLBP, CLBC, CLTP and WCLTP) are presented. Additionally, three different experiments were performed to evaluate the effectiveness of LBP and its variants descriptors for rotation, illumination and scale invariant texture classification using three well-known texture benchmark datasets (i.e. OuTeX, CURET and UIUC). The main goal of this paper is to find a superior LBP-based descriptor that

performs powerfully for texture classification. The empirical experimental results showed that the WCLTP outperformed other LBP variants. The rest of this paper is organized as follows. Section 2 explains the LBP in detail, while section 3 briefly reviews the variants of LBP. Section 4, shows the experimental results Finally, Section 5 concludes the paper.

2. LOCAL BINARY PATTERN (LBP)

The initial LBP method proposed by Ojala et al. [10] was used to extract a texture feature. It provides the local measure of image contrast. LBP has initially been defined within the concept of 8 pixels and grey value centre pixel. The grey level variance between the centre pixel and its neighbourhood pixel is calculated. The neighbourhood pixels is set to 1 if the variance is positive or 0 if it's negative; then, these values are used to obtain a binary code which is generated later to represent a histogram that describes the image texture. Figure 1 showed the process of calculation in the original LBP. The LBP was developed by Ojala et al. [14] based on the use of differently sized neighbourhoods with the aid of a symmetric circle neighbourhood defined by R and P. Mathematically, LBP is defined as:

$$LBP_{P,R} = \sum_{p=0}^{P-1} 2^p s(i_p - i_c), s(x) = \begin{cases} 1, & x \geq 0 \\ 0, & x < 0 \end{cases} \quad (1)$$

Where i_c and i_p point out to the grey values of the centre pixel and the neighbour pixel, and R represents the radius of the circle. P is the number of neighbourhood pixels. The neighbours' pixels that do not fall exactly in the centre of pixels are estimated by interpolation. LBP is called uniform if its uniformity measure is equal to at most 2. Uniformity (U) is the number of bitwise transitions from 0 to 1 or 1 to 0 when the bit pattern is considered circular. For example, patterns 11111111, 10001111, and 01010011 have 0, 2 and 6 transitions, respectively. The first two patterns are uniform since the uniformity measure is 2 or less, and the third pattern is non-uniform since it consists of more than two transitions. In uniform pattern LBP, each pattern will be assigned by a separate label, and all non-uniform patterns will be assigned to a single label. This makes the uniform pattern LBP $LBP_{P,R}^{u2}$ histogram size smaller compared to the original LBP. With uniform patterns, for P neighbours, there will be $P*(P-1)+3$: different texture features as opposed to 2^P features in the original LBP. To achieve rotation invariance, a locally

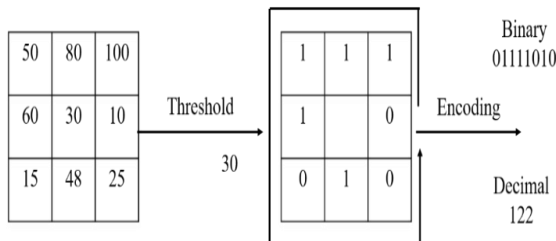


Figure 1: LBP operator

rotation invariant pattern is presented as:

$$LBP_{P,R}^{riu2} = \begin{cases} \sum_{p=0}^{P-1} 2^p s(i_p - i_c) & \text{if } U(LBP_{P,R}) \leq 2 \\ p + 1 & \text{otherwise} \end{cases} \quad (2)$$

The mapping from $LBP_{P,R}$ to $LBP_{P,R}^{riu2}$ [14], which has p+2 distinct output values, can be implemented with a lookup table. There are two main weaknesses in the LBP; the first one is its sensitivity to noise and the second is that sometimes, the different patterns of LBP may be classified into the same class. These weaknesses can be shown in Figure 2 and Figure 3.

3. LOCAL BINARY PATTERN VARIANTS

In this section, a brief review of the most significant LBP variants, namely: Local Ternary Pattern (LTP) [15], Completed Local Binary Pattern (CLBP), Completed Local Binary Count (CLBC), Completed Local Ternary Pattern (CLTP), and Wavelet Completed Local Ternary Pattern (WCLTP) were provided.

3.1 Local Ternary Pattern

In 2010, Tan and Triggs [15] modified the general LBP model with a view to overcoming the sensitivity-to-noise issue by adding a threshold value (t) and encoding the neighbour pixel values into 3-value instead of 2-valued codes. The new version was called the Local Ternary Pattern (LTP), mathematically presented as follows:

$$LTP_{P,R} = \sum_{p=0}^{P-1} 2^p s(i_p - i_c), s(x) = \begin{cases} 1, & t \geq 0 \\ 0, & -t < x < t \\ -1, & x < -t \end{cases} \quad (3)$$

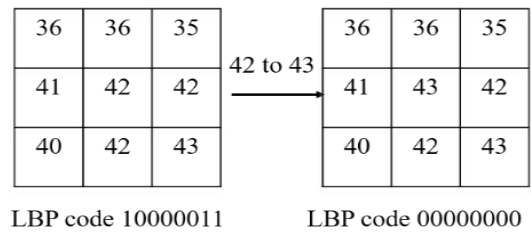


Figure 2: An example of the LBP operator's noise sensitivity

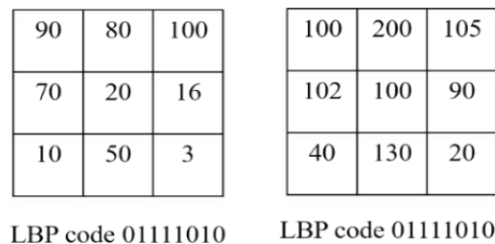


Figure 3: An example of similar LBP codes for two different texture patterns.

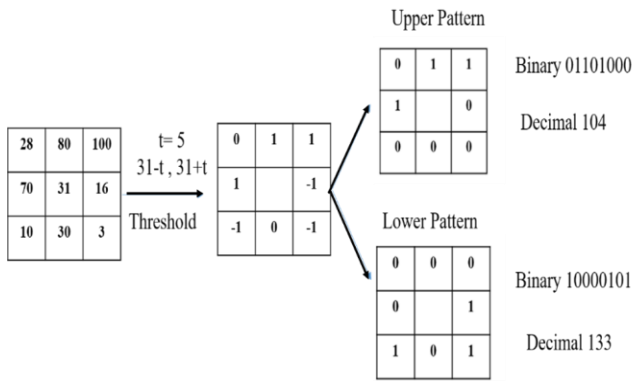


Figure 4: LTP operator

where i_c , i_p , R , and P are defined previously in (1), and t indicate the threshold value. Figure 4 illustrates the LTP encoding process. LTP is robust to noise but it is no longer invariant to monotonic grey scale transformation.

3.2 Completed Local Binary Pattern

Guo et al [16] proposed the completed LBP. In the CLBP, the image local differences are divided into two complementary components (sign (s_p) and magnitude (m_p)) which are used to build CLBP_Sign (CLBP_S) and CLBP_Magnitude (CLBP_M), respectively. They can be expressed as follows:

$$CLPB_{S_{P,R}} = \sum_{p=0}^{P-1} 2^p s(i_p - i_c), s(p) = \begin{cases} 1, & i_p \geq i_c \\ 0, & i_p < i_c \end{cases} \quad (4)$$

$$CLPB_{M_{P,R}} = \sum_{p=0}^{P-1} 2^p t(m_p, c), t(m_p, c) = \begin{cases} 1, & |i_p - i_c| \geq c \\ 0, & |i_p - i_c| < c \end{cases} \quad (5)$$

where i_c , i_p , R , and P are defined in (1), and c denotes the mean value of m_p . Figure 5 shows an example of calculating the sign and magnitude of CLBP. Guo et al [16] observed that the centre pixel also has discriminative information. So, they defined an operator CLBP_C to extract the local central information. CLBP_C was defined as:

$$CLBP_{C_{P,R}} = t(i_c, c_l) \quad (6)$$

where i_c denotes the grey value of the centre pixel of the pattern, and C_l denotes the average grey level of the entire image. Guo et al. combined their operators into joint or hybrid distributions and achieved a remarkable texture classification accuracy. The CLBP suffers from three main problems, the

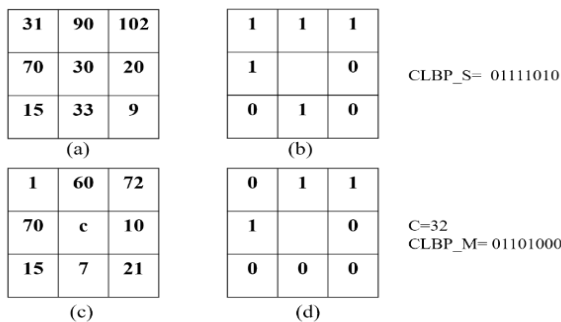


Figure 5: (a) a 3×3 pattern. (b) CLBP_S. (c) magnitude component. (d) CLBP_M

first one is that the dimensionality of the CLBP_M has the same size of the CLBP_S which means there is a sharp growth in the size of the histogram. Furthermore, the complementary between the sign component and the magnitude component should be exploited [17], in addition to the noise sensitivity problem.

3.3 Completed Local Binary Count

In 2012, Y. Zhao et al [18] proposed a new scheme called Local Binary Count (LBC) for rotation invariant classification. Unlike the LBP and its variants, the concept of LBC depends on counting the number of values 1's that resulted from the thresholding step without doing the encoding step. An example of LBC operator is shown in Figure 6. LBC can be described mathematically as follows:

$$LBC_{P,R} = \sum_{p=0}^{P-1} s(i_p - i_c), s(x) = \begin{cases} 1, & x \geq 0 \\ 0, & x < 0 \end{cases} \quad (7)$$

Influenced by CLBP [16], the authors developed the LBC to completed LBC (CLBC). Similar to CLBP, the three operators, CLBC_S, CLBC_M, and CLBC_C were also combined into joint or hybrid distributions. The CLBC_S is equal to the original LBC that was described above in (7). The CLBC_M and CLBC_C can be described mathematically as follows:

$$CLPC_{M_{P,R}} = \sum_{p=0}^{P-1} 2^p t(m_p, c), t(m_p, c) = \begin{cases} 1, & |i_p - i_c| \geq c \\ 0, & |i_p - i_c| < c \end{cases} \quad (8)$$

$$CLBC_{C_{P,R}} = t(i_c, c_l) \quad (9)$$

where i_c , i_p , R , P , C and c_l are defined in (1), (4), and (5). The three operators are combined into joint or hybrid distributions and used to extract the texture features which are rotation invariants. The CLBC can achieve similar accurate classification rates as CLBP; however, it reduces the computational complexity that is needed in the training and classification process. In term of limitation, the CLBC also suffers from the same CLBP limitations [19].

3.4 Completed Local Ternary Pattern

Rassem and Bee [19] proposed the CLTP by combining the CLBP [16] and LTP [15] operators. In CLTP, the local difference of the image is divided into two sign complementary components and two magnitude complementary components as follows:

$$S_p^{upper} = S(i_p - (i_c + t)), S_p^{lower} = S(i_p - (i_c - t)) \quad (10)$$

$$M_p^{upper} = |i_p - (i_c + t)|, M_p^{lower} = |i_p - (i_c - t)| \quad (11)$$

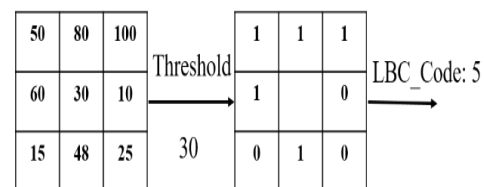


Figure 6: LBC operator

Where i_c, i_p and t are described in (1) and (2). Then the sign components are used to build the $CLTP_{P,R}^{upper}$ and $CLTP_{P,R}^{lower}$, as follows:

$$CLTP_{P,R}^{upper} = \sum_{p=0}^{P-1} 2^p s(i_p - (i_c + t)), S_p^{upper} = \begin{cases} 1, & i_p \geq i_c + t, \\ 0, & \text{otherwise,} \end{cases} \quad (12)$$

$$CLTP_{P,R}^{lower} = \sum_{p=0}^{P-1} 2^p s(i_p - (i_c - t)), S_p^{lower} = \begin{cases} 1, & i_p < i_c - t, \\ 0, & \text{otherwise,} \end{cases} \quad (13)$$

The two operators then are concatenated to form $CLTP_{P,R}$ as follows:

$$CLTP_{P,R} = [CLTP_{P,R}^{upper} \quad CLTP_{P,R}^{lower}] \quad (14)$$

Likewise, to $CLTP_{P,R}$, the $CLTP_{M,P,R}$ is built using the two magnitude complementary components m_p^{upper} and m_p^{lower} as follows:

$$CLTP_{M,P,R}^{upper} = \sum_{p=0}^{P-1} 2^p t(m_p^{upper}, c), t(m_p^{upper}, c) = \begin{cases} 1, & |i_p - (i_c + t)| \geq c, \\ 0, & |i_p - (i_c + t)| < c, \end{cases} \quad (15)$$

$$CLTP_{M,P,R}^{lower} = \sum_{p=0}^{P-1} 2^p t(m_p^{lower}, c), t(m_p^{lower}, c) = \begin{cases} 1, & |i_p - (i_c - t)| \geq c, \\ 0, & |i_p - (i_c - t)| < c, \end{cases} \quad (16)$$

$$CLTP_{M,P,R} = [CLTP_{M,P,R}^{upper} \quad CLTP_{M,P,R}^{lower}] \quad (17)$$

Similar to that, the $CLTP_{C,P,R}^{upper}$ and $CLTP_{C,P,R}^{lower}$ can be mathematically expressed as follows:

$$CLTP_{C,P,R}^{upper} = t(i_c^{upper}, C_I) \quad (18)$$

$$CLTP_{C,P,R}^{lower} = t(i_c^{lower}, C_I) \quad (19)$$

where $i_c^{upper} = i_c + t$, $i_c^{lower} = i_c - t$ and C_I is the average grey level of the whole image. Finally, operator histogram CLTP is Figure 7: An example of CLTP operator constructed by the combination of these three operators into joint or hybrid distributions similar to the CLBP [16] and CLBC[18], respectively. The final histogram is double in size compared with the CLBP histogram which is may consider as a weak point in this operator. Fig. 8 shows an example of CLTP calculations. In this example, the threshold value is set to 5 and used to find the upper and lower values for the centre pixel; the new centre pixel values 39 and 29 are subtracted from the neighbours to find new upper and lower patterns. The $CLTP_S$ (upper) and $CLTP_S$ (lower) are thresholded using the upper and lower values of centre pixels, while the $CLTP_M$ (upper) and $CLTP_M$ (lower) are calculated based on the mean value of the neighbour pixels in the upper and lower patterns.

3.5 Wavelet Completed Local Ternary Pattern

In 2017, a new texture descriptor inspired by CLTP was proposed called WCLTP [20] WCLTP improves the classification accuracy of CLTP by incorporating it with a Redundant Discrete Wavelet Transform (RDWT) [21]. Extracting CLTP in wavelet transform will help to increase

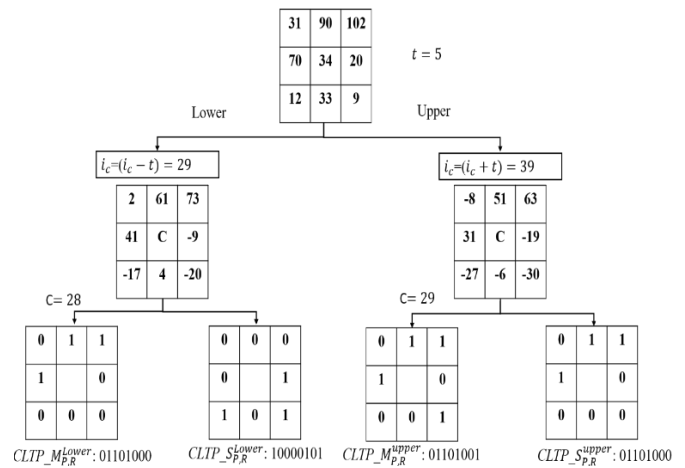


Figure 7: An example of CLTP operator

the classification accuracy due to the shift invariant property of RDWT. Firstly, the image is decomposed into four sub-bands (LL, LH, HL, HH). Then, the LL wavelet coefficients are used to extract CLTP and build the three WCLTP operators (i.e. WCLTP_S, WCLTP_M and WCLTP_C). RDWT is unlike the discrete wavelet transform (DWT) where the sub-band size is only half the size of the image. As a result, the important textures in the image will be at the same spatial location in each sub-band. Figure 8 summarized the extraction of WCLTP. The WCLTP operators are combined into joint or hybrid distributions to build the final operator histogram like the CLTP. The operators of the same type of pattern; i.e., the upper and the lower pattern, are combined first into joint or hybrid distributions; then, their results are concatenated to build the final operator histogram. The WCLTP inherits the high dimensionality problem from the CLTP. The strengths and drawbacks of LBP and its variants are presented in Table 1. The table shows the limitations of the original LBP and some of its variants. Although most LBP variants aimed to handle the limitations of LBP, they still inherited at least one of LBP's limitations, (i.e. sensitivity to noise, rotation variant, Using tuning parameter, computational complexity and high dimensionality).

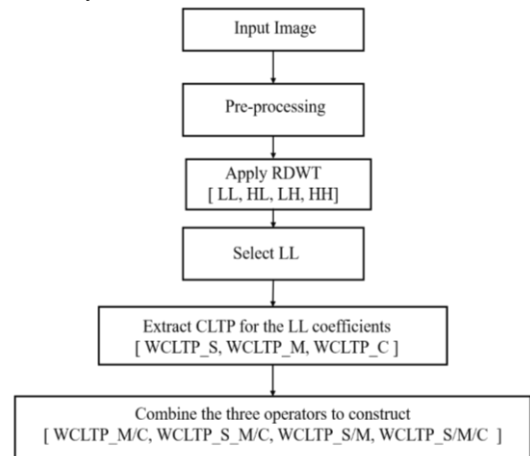


Figure 8: Flowchart of WCLTP extraction process

Table 1: The limitations of LBP and its variants.

Descriptor	Ref.	Year	Limitations					Histogram size
			Noise sensitivity	Rotation sensitivity	Using tuning parameter	Computational complexity	Dimensionality	
LBP	[10]	1996	Yes	Yes	No	No	Yes	2^P
$LBP_{P,R}^{pi}$	[14]	2002	Yes	No	No	No	Yes	2^P
$LBP_{P,R}^{pi2}$	[14]	2002	Yes	No	No	No	Yes	$P(P-1)+3$
$LBP_{P,R}^{riu2}$	[14]	2002	Yes	No	No	No	No	$P+2$
LTP	[15]	2010	Yes	No	Yes	No	No	$(p+2)*2$
CLBP	[16]	2010	Yes	No	No	Yes	Yes	$(p+2)(p+2)*2$
CLBC	[18]	2012	Yes	No	No	Yes	Yes	$(p+1)(p+1)*2$
CLTP	[19]	2014	No	No	Yes	Yes	Yes	$((P+2)*(P+2)*2)*2$
WCLTP	[20]	2017	No	No	Yes	Yes	Yes	$((P+2)*(P+2)*2)*2$

Yes, indicates the limitation still exists
 No indicates the limitation has been overcome.

Dimensionality is considered a significant problem in most LBP variants. The high dimensionality increases the computational complexity of the descriptor and slows down the classification process. Based on the table, most variants of LBP are susceptible to the dimensionality issue. The $LBP_{P,R}^{riu2}$ has the least dimensionality size while CLTP and WCLTP have the largest size.

4. EXPERIMENTS AND DISCUSSION

To evaluate the performance of LBP variants, three types of empirical experiments were executed. The first experiment was performed on the Outex texture dataset (TC10) and (TC12) [22]. The second experiment was performed using the Columbia-Utrecht Reflection and Texture database CURET [23].The UIUC database. [24].

4.1 Dissimilarity Measuring Framework

In this paper, the chi-square statistic metric is used to check the dissimilarity between two histograms whereas the nearest neighbourhood classifier is used in classification. The following equation calculates the distance x^2 between two histogram $H = h_i$ and $K = k_i$ where $(i = 1,2,3,4,...,B)$:

$$Dissimilarity_{x^2}(H,K) = \sum_{i=1}^B \frac{(h_i - k_i)^2}{h_i + k_i} \quad 20$$

4.2 Experimental Results on OuTeX Database

The Outex dataset contains 16 suits; in our experiment, OuTeX -TC-0010 and OuTeX -TC-0012 were selected as they were two well-known test suites. Each of them includes 24 classes of texture images which were taken under 3 illuminations ("inca") for TC-0010 and ("t184" and "horizon") for TC-0012, and 9 rotation angles (0°, 5°, 10°, 15°, 30°, 45°, 60°, 75°, and 90. For TC10, the 24 x 20 samples of illuminant "inca" and rotation 0° in each class were used for training the classifier, while the rest of the rotation angles were used for testing. For TC12, the same training samples as TC10 were used for classifier training. The whole sample in TC-0012 taken under lighting "t184" and "horizon" was

adopted as a testing sample. Table 2 showed the experimental results of TC10, TC12(t184), and TC12 (horizon).

The table showed that a high classification rate was achieved when the three operators (S/M/C) were joined. The WCLTP outperformed other LBP variants in all experiments and achieved the highest accuracy rate of 99.35% for (P = 24 and R = 3). This implied its robustness to illumination changes. CLBP_S/M and CLTP_S/M followed with 99.32% and 99.04% accuracy rates, respectively for the same pattern size. The LBP on the performance; in some cases, the improvement exceeded 13% by only a change in the pattern type. The CLTP showed competitive results compared to WCLTP; in some cases, it had about 2% higher classification accuracy than WCLTP. For example, CLTP_S achieved 96.95% on TC10 for (P = 16, R = 2) while WCLTP_S achieved 94.97%.

4.3 Experimental results on CURET database

The CURET dataset consists of 61 texture classes with 205 images for each class captured from several viewpoints and lighting direction. 118 images out of 205 images are shot from a viewing angle of less than 60°. From these 118, only 92 images were selected and converted to grayscale before cropping to 200 x 200. In each class, the selected 92 images were divided into two groups; the first group contained N number of images which were selected randomly and used as training images (N = 6, 12, 23, 46). The second group contained the remaining (92-N) images which were used as testing data. The final classification accuracy was the average percentage of over a hundred random splits. The performance of the LBP variants on CURET database was shown in Table 3. From the table, similar findings were observed. The highest classification accuracy was 96.57% which was achieved by WCLTP_S/M/C for (P = 24 and R = 3), followed by 96.11% and 95.39% which achieved by CLBP_S/M/C and CLBC_S/M/C, for the same pattern. In some cases, CLTP showed superior performance, especially when using a smaller number of training samples. For example, CLTP S/M/C had 2% higher accuracy than WCLTP_S/M/C for (R = 3 and P = 25) when the training samples were 6, while the difference did not exceed 0.01% when the training samples were 46. In some other cases, WCLTP showed better

Table 2: Classification rates (%) on TC10 and TC12 databases.

Descriptor	Parameters (R,P) . R =the radius of the circle, P =the number of neighbourhood pixels											
	P=8, R=1				P=16, R=2				P=24, R=3			
	TC10	TC12		Average	TC10	TC12		Average	TC10	TC12		Average
		"t"	"h"			"t"	"h"			"t"	"h"	
LBPriu2	84.87	65.19	64.03	71.36	89.40	82.48	75.30	82.39	95.16	85.05	80.88	87.03
LTP	94.14	75.88	73.96	81.33	96.95	90.16	86.94	91.35	98.2	93.59	89.42	93.74
CLBP_S	84.81	65.46	63.68	71.32	89.40	82.26	75.20	82.29	95.07	85.04	80.78	86.96
CLBC_S	82.94	65.02	63.17	70.38	88.67	82.57	77.41	82.88	91.35	83.82	82.75	85.97
CLTP_S	94.14	75.88	73.96	81.33	96.95	90.16	86.94	91.35	98.20	93.59	89.42	93.74
WCLTP_S	92.97	83.56	80.00	85.51	94.97	92.04	86.81	91.27	97.89	93.87	90.51	94.09
CLBP_M	81.74	59.31	62.77	67.94	93.67	73.79	72.40	79.95	95.52	81.18	78.65	85.12
CLBC_M	78.96	53.63	58.01	63.53	92.45	70.35	72.64	78.48	91.85	75.59	74.58	80.67
CLTP_M	94.04	75.86	74.05	81.32	97.32	83.40	84.40	88.37	98.00	85.39	84.65	89.35
WCLTP_M	94.51	77.36	77.71	83.19	97.11	82.71	86.53	88.78	97.89	83.54	84.42	88.62
CLBP_M/C	90.36	72.38	76.66	79.80	97.44	86.94	90.97	91.78	98.02	90.74	90.69	93.15
CLTP_M/C	95.94	84.70	86.02	88.89	97.94	90.14	92.38	93.49	98.52	91.23	89.98	93.24
WCLTP_M/C	95.86	85.56	87.59	89.67	97.99	91.46	93.43	94.29	98.44	92.29	93.08	94.60
CLBP_S_M/C	94.53	81.88	82.52	86.31	98.02	90.99	91.08	93.36	98.33	94.05	92.40	94.93
CLTP_S_M/C	96.43	84.00	86.85	89.09	98.44	92.41	92.80	94.55	98.98	95.00	92.94	95.64
WCLTP_S_M/C	97.27	88.98	89.26	91.84	97.94	93.63	92.94	94.84	98.78	95.56	94.40	96.24
CLBP_S/M	94.66	82.75	83.14	86.85	97.89	90.55	91.11	93.18	99.32	93.58	93.35	95.42
CLBC_S/M	95.23	82.13	83.59	86.98	98.10	89.95	90.42	92.82	98.70	91.41	90.25	93.45
CLTP_S/M	96.41	82.85	84.81	88.02	97.84	92.06	92.69	94.20	99.04	94.14	95.59	96.26
WCLTP_S/M	96.54	86.97	86.62	90.04	98.44	93.68	93.01	95.04	99.35	94.75	94.14	96.08
CLBP_S/M/C	96.56	90.30	92.29	93.05	98.72	93.54	93.91	95.39	98.93	95.32	94.53	96.26
CLBC_S/M/C	97.16	89.79	92.92	93.29	98.54	93.26	94.07	95.29	98.78	94.00	93.24	95.34
CLTP_S/M/C	96.88	90.25	92.92	93.35	98.83	93.59	94.26	95.56	99.17	95.67	94.28	96.37
WCLTP_S/M/C	98.13	91.25	93.32	93.56	98.80	95.60	95.19	96.53	99.22	96.76	95.77	97.25

Table 3: Classification rates (%) on CURET databases

Descriptor	Parameters (R,P) . R =the radius of the circle, P =the number of neighbourhood pixels											
	P=8, R=1				P=16, R=2				P=24, R=3			
	6	12	23	46	6	12	23	46	6	12	23	46
LBPriu2	60.36	69.05	74.64	81.32	63.38	72.70	79.28	84.53	67.86	75.51	81.65	86.35
LTP	62.01	71.63	80.07	86.74	67.72	77.11	86.39	91.42	70.15	78.86	86.41	92.44
CLBP_S	58.70	67.84	74.81	80.63	66.17	74.62	81.05	86.37	66.55	74.71	81.12	86.37
CLBC_S	56.88	66.21	72.89	78.82	60.42	68.95	74.42	79.78	60.82	70.57	74.21	80.14
CLTP_S	64.38	72.66	81.73	88.24	68.39	79.09	86.61	91.55	72.57	81.55	87.72	91.75
WCLTP_S	62.73	72.18	79.48	85.90	68.54	78.47	83.17	89.16	70.50	78.68	85.20	90.57
CLBP_M	51.49	60.27	67.96	75.20	61.59	71.24	79.01	85.48	60.45	69.22	76.23	82.16
CLBC_M	50.12	58.62	57.82	66.61	50.63	58.70	66.05	73.89	51.23	60.53	68.36	77.41
CLTP_M	61.37	71.17	80.53	86.67	63.33	74.47	82.14	88.83	67.14	76.93	85.16	90.52
WCLTP_M	58.22	67.94	76.14	83.74	64.49	72.82	82.19	88.00	64.89	74.86	82.89	89.11
CLBP_M/C	56.45	66.91	75.58	83.26	68.14	78.05	85.73	91.42	66.41	75.96	83.54	89.48
CLTP_M/C	62.07	72.94	82.26	88.98	66.77	77.12	85.51	91.67	70.10	80.12	89.02	93.58
WCLTP_M/C	61.83	73.01	81.68	88.96	66.61	77.96	86.43	92.52	71.55	80.99	88.20	93.60
CLBP_S_M/C	66.31	76.42	84.52	90.34	72.51	82.46	89.05	93.87	72.01	81.44	88.37	93.22
CLTP_S_M/C	67.54	78.89	85.46	91.27	71.55	82.16	87.82	94.04	74.36	85.14	91.03	94.69
WCLTP_S_M/C	67.70	77.89	86.81	92.63	70.12	83.44	88.94	94.06	74.55	83.37	90.34	94.87
CLBP_S/M	72.30	81.95	88.67	93.52	75.39	84.17	90.40	94.45	73.26	82.47	89.14	93.63
CLBC_S/M	69.89	79.88	86.62	93.10	72.16	81.71	89.60	93.78	70.52	81.57	89.12	93.60
CLTP_S/M	71.30	82.37	89.20	93.50	74.14	84.42	90.78	95.06	76.49	85.11	90.02	95.63
WCLTP_S/M	70.63	81.67	88.46	93.69	75.79	84.87	90.87	95.49	76.31	85.25	91.59	95.43
CLBP_S/M/C	74.80	84.92	91.35	95.59	77.04	86.15	92.13	95.86	74.46	83.82	90.33	94.74
CLBC_S/M/C	72.85	82.92	90.12	94.78	75.17	85.91	91.30	95.39	73.18	84.07	90.55	95.26
CLTP_S/M/C	75.18	84.06	90.45	94.78	75.17	85.54	92.44	95.95	77.97	87.50	92.72	96.11
WCLTP_S/M/C	72.81	83.96	91.10	95.86	77.85	86.68	92.53	96.27	78.30	87.27	93.28	96.57

performance, especially when using (R = 2 and P = 16) pattern type. The best accuracy for this pattern size was 95.86% which recorded by WCLTP, followed by 95.59% for CLBP_S/M/C, and 94.78% for both CLBC_S/M/C and CLTP_S/M/C.

4.4 Experimental results on UIUC database

The UIUC dataset includes 25 texture classes. Each class has 40 images captured in different illumination conditions and viewing points. Figure 12 showed examples of UIUC images. Different training images (N) are randomly selected for each class where (N = 5, 10, 15, 20). The remaining (40-N) images are used as the test data. Each random selection is repeated 100 times to obtain statistically valid experimental results. The experimental results of the UIUC dataset are shown in Table 4. A significant observation that can be drawn from the table is that the UIUC dataset is difficult for most descriptors especially when using a single operator. Most variants such as LTP, CLBP and CLBC achieved classification accuracy less than 60% in single operator and less than 50% in some case because of the complex characteristics of the data, such as high resolution and nonrigid deformations. WCLTP shows on average the best performance compared with other methods in all cases. WCLTP achieved the highest accuracy rate of 94.80% when integrating the three operators together WCLTP_S/M/C24,3. In some cases when (R = 2 and 3), CLTP_M and CLTP_M/C performed better than WCLTP_M and WCLTP_M/C, respectively.

5. CONCLUSION

Table 4. Classification rates (%) on the UIUC Dataset

Method	Parameters (R,P) . R =the radius of the circle, P =the number of neighbourhood pixels											
	(R=1,P=8)				(R=2,P=16)				(R=3,P=24)			
	5	10	15	20	5	10	15	20	5	10	15	20
LTP	50.06	58.27	64.64	67.80	61.26	71.33	74.40	78.20	60.91	74.53	78.72	83.40
CLBP_S	40.05	47.53	51.63	55.29	41.80	51.34	56.80	60.60	44.87	54.68	60.63	64.20
CLBC_S	39.85	46.69	51.11	55.61	43.37	53.07	59.17	62.39	47.19	57.46	63.48	66.90
CLTP_S	54.29	61.87	69.92	71.60	64.91	75.07	80.48	83.20	68.80	77.60	83.04	86.00
WCLTP_S	61.65	71.53	76.01	78.61	69.45	78.28	82.53	85.06	72.91	81.15	84.80	87.01
CLBP_M	42.39	49.98	54.45	57.52	56.07	65.65	69.51	72.05	56.15	65.92	71.05	74.37
CLBC_M	39.04	45.51	49.42	52.12	50.67	59.01	64.42	67.10	51.68	60.62	66.63	69.33
CLTP_M	57.49	64.67	69.60	73.60	70.29	79.33	83.36	85.40	69.94	79.33	82.56	85.20
WCLTP_M	66.19	74.00	77.97	80.28	70.25	77.97	81.80	83.49	69.43	76.83	80.42	82.85
CLBP_M/C	56.92	65.09	69.81	72.66	68.45	76.83	80.14	82.72	68.08	76.75	80.81	83.27
CLTP_M/C	70.06	76.93	80.48	81.80	77.37	83.60	87.04	89.40	76.80	83.47	87.20	88.60
WCLTP_M/C	69.82	77.33	81.50	83.76	75.42	82.75	86.08	87.76	76.15	83.21	86.58	88.41
CLBP_S_M/C	62.52	71.27	75.48	78.65	68.68	77.57	81.36	83.55	69.43	78.61	82.81	85.33
CLTP_S_M/C	68.80	77.33	80.48	83.60	77.37	84.27	87.84	89.80	77.26	84.67	88.48	90.60
WCLTP_S_M/C	72.87	80.24	83.59	86.06	79.05	85.66	89.07	90.77	79.92	86.61	89.58	91.09
CLBP_S/M	64.70	74.65	79.55	82.58	71.80	80.85	85.31	87.60	72.05	82.63	86.88	89.56
CLBC_S/M	65.28	74.88	78.86	82.40	73.16	82.04	86.31	88.51	75.16	83.92	87.68	89.72
CLTP_S/M	65.03	74.40	79.68	83	77.14	85.60	89.44	91.80	79.31	87.73	90.56	93.20
WCLTP_S/M	74.99	82.32	86.12	88.02	82.51	89.15	91.55	92.87	83.80	89.92	92.27	93.80
CLBP_S/M/C	74.53	82.26	85.85	87.86	78.75	86.33	89.25	91.03	78.05	85.87	89.17	91.07
CLBC_S/M/C	74.57	82.35	85.66	87.83	79.48	86.63	89.66	91.04	79.75	86.45	90.10	91.39
CLTP_S/M/C	74.51	81.73	85.92	86.80	82.63	87.87	90.40	92.60	82.97	88.93	91.52	94.40
WCLTP_S/M/C	77.55	84.72	87.68	89.28	84.21	90.11	92.28	93.48	84.63	90.22	92.72	94.80

This paper examined the limitations and performances of six texture classification descriptors (LBP, LTP, CLBP, CLBC, CLTP, and WCLTP) using three benchmarks datasets (CURET OuTeX and UIUC). The evaluations showed that most LBP variants can improve classification accuracies but can also cause an increase in histogram dimensionality. High dimensionality negatively affected the performance of the descriptor and increased the running time. Moreover, high dimensionality needs large storage space. Furthermore, a comparison of the descriptors in term of results was performed, and from the empirical results, showed that WCLTP outperformed the other descriptors in terms of classification accuracy and exhibited significant resistance to noise and illumination variations. However, WCLTP suffers from the high dimensionality where the size of the resultant histogram is too large. Therefore, further studies are needed to improve the LBP descriptor and its variants, with a special focus on reducing their dimensionality size and enhancing the classification accuracy.

ACKNOWLEDGEMENT

The first named author is grateful to Universiti Malaysia Pahang for providing Master Research Scheme (MRS) fellowship. This work is supported by the Universiti Malaysia. Pahang (UMP) via Research Grants PGRS190381 and RDU 180365.

REFERENCES

1. T. H. Rassem, B. E. Khoo, M. F. Mohammed, and N. M. Makbol, "Medical, scene and event image category recognition using completed local ternary patterns

- (CLTP),” *Malaysian J. Comput. Sci. (ISSN 0127-9084)*, vol. 30, no. 3, pp. 200–218, 2017.
2. P. Thakur and R. Shrivastava, “**A Review on Text Based Emotion Recognition System,**” *International Journal of Advanced Trends in Computer Science and Engineering*, vol. 7, no. 5, pp. 67-71, 2018.
 3. T. H. Rassem, N. M. Makbol, and S. Y. Yee, “**Face recognition using completed local ternary pattern (CLTP) texture descriptor,**” *Int. J. Electr. Comput. Eng.*, vol. 7, no. 3, p. 1594, 2017.
 4. D. Sarala, T. Kanikdaley, S. Jogi, and R. K. Chaurasiya, “**Content-based image retrieval using hierarchical color and texture similarity calculation,**” *International Journal of Advanced Trends in Computer Science and Engineering*, vol. 7, pp. 11-16, 2018.
 5. L. Liu, J. Chen, P. Fieguth, G. Zhao, R. Chellappa and M. Pietikäinen, “**From BoW to CNN: Two Decades of Texture Representation for Texture Classification**” *International Journal of Computer Vision*, vol. 127, pp. 74–109, 2019
 6. R. Maani, S. Kalra, and Y.-H. Yang, “**Noise robust rotation invariant features for texture classification,**” *Pattern Recognit.*, vol. 46, no. 8, pp. 2103–2116, 2013.
 7. Y. Xu, Y. Quan, H. Ling, and H. Ji, “**Dynamic texture classification using dynamic fractal analysis,**” in *Computer Vision (ICCV), 2011 IEEE International Conference on*, 2011, pp. 1219–1226.
 8. W. Gu, Z. Lv, and M. Hao, “**Change detection method for remote sensing images based on an improved Markov random field,**” *Multimed. Tools Appl.*, vol. 76, no. 17, pp. 17719–17734, 2017.
 9. D. R. Nayak, R. Dash, and B. Majhi, “**Brain MR image classification using two-dimensional discrete wavelet transform and AdaBoost with random forests,**” *Neurocomputing*, vol. 177, pp. 188–197, 2016.
 10. T. Ojala, M. Pietikäinen, and D. Harwood, “**A comparative study of texture measures with classification based on featured distributions,**” *Pattern Recognit.*, vol. 29, no. 1, pp. 51–59, 1996.
 11. M. Pietikäinen, A. Hadid, G. Zhao, and T. Ahonen, “**Computer vision using local binary patterns,**” *Springer Science & Business Media, 2011*. vol. 40
 12. L. Nanni, S. Brahmam, and A. Lumini, “**A local approach based on a Local Binary Patterns variant texture descriptor for classifying pain states,**” *Expert Syst. Appl.*, vol. 37, no. 12, pp. 7888–7894, 2010.
 13. D. Huang, C. Shan, M. Ardabilian, Y. Wang, and L. Chen, “**Local binary patterns and its application to facial image analysis: a survey,**” *IEEE Trans. Syst. Man, Cybern. Part C.*, vol. 41, no. 6, pp. 765–781, 2011.
 14. T. Ojala, M. Pietikäinen, and T. Maenpää, “**Multiresolution Gray Scale and Rotation Invariant Texture Classification with Local Binary Patterns,**” *IEEE Trans. Pattern Anal. Mach.*, vol. 24, pp. 971–987, 2002.
 15. X. Tan and B. Triggs, “**Enhanced local texture feature sets for face recognition under difficult lighting conditions,**” *IEEE Trans. Image Process.*, vol. 19, no. 6, pp. 1635–1650, 2010.
 16. Z. Guo, L. Zhang, and D. Zhang, “**A completed modeling of local binary pattern operator for texture classification,**” *IEEE Trans. Image Process.*, vol. 19, no. 6, pp. 1657–1663, 2010.
 17. C. S. Sree, “**Survey on Extraction of Texture based Features using Local Binary Pattern,**” *Int. J. Eng. Res. Technol.*, vol. 4, no. 7, pp. 334–338, 2015.
 18. Y. Zhao, D. S. Huang, and W. Jia, “**Completed local binary count for rotation invariant texture classification,**” *IEEE Trans. Image Process.*, vol. 21, no. 10, pp. 4492–4497, 2012.
 19. T. H. Rassem and B. E. Khoo, “**Completed local ternary pattern for rotation invariant texture classification,**” *Sci. World J.*, vol. 2014.
 20. A. Shamaileh, T. H. Rassem, I. A. Ahmed, and K. M. Alalayah, “**Wavelet Completed Local Ternary Pattern (WCLTP) for Texture Image Classification,**” in *The 5th International Conference on Software Engineering & Computer System (ICSECS’ 17)*, 2017, pp. 83–89.
 21. J. E. Fowler, “**The redundant discrete wavelet transform and additive noise,**” *IEEE Signal Process. Lett.*, vol. 12, no. 9, pp. 629–632, 2005.
 22. T. Ojala, T. Maenpää, M. Pietikäinen, J. Viertola, J. Kyllönen, and S. Huovinen, “**Outex-new framework for empirical evaluation of texture analysis algorithms,**” in *Pattern Recognition, 2002. Proceedings. 16th International Conference on*, 2002, vol. 1, pp. 701–706.
 23. K. J. Dana, B. Van Ginneken, S. K. Nayar, and J. J. Koenderink, “**Reflectance and texture of real-world surfaces,**” *ACM Trans. Graph.*, vol. 18, no. 1, pp. 1–34, 1999.
 24. Lazebnik, S., Schmid, C., & Ponce, J., “**A sparse texture representation using local affine regions,**” *IEEE Transactions on Pattern Analysis and Machine Intelligence*, vol. 27, pp. 1278–34, 2005.